

RESEARCH

Open Access



# FOSB is a key factor in the genetic link between inflammatory bowel disease and acute myocardial infarction: multiple bioinformatics analyses and validation

Qingan Fu<sup>1†</sup>, Tianzhou Shen<sup>1†</sup>, Weihan Qiu<sup>2†</sup>, Yanhui Liao<sup>1</sup>, Miao Yu<sup>1\*</sup> and Yue Zhou<sup>1\*</sup>

## Abstract

**Background** Inflammatory Bowel Disease (IBD), which includes Crohn's disease and ulcerative colitis, is associated with an increased risk of Acute Myocardial Infarction (AMI). The genetic mechanisms underlying this link are not well understood.

**Methods** We downloaded IBD and AMI-related microarray datasets from the NCBI Gene Expression Omnibus (GEO) database. Differentially expressed genes (DEGs) were identified and analyzed using enrichment analysis and Weighted Gene Co-expression Network Analysis (WGCNA). Machine learning techniques, including LASSO, random forest, and Boruta, were employed to screen for hub genes. These genes were validated through qRT-PCR and Western blotting. Single-cell sequencing was used to confirm findings. Additionally, potential therapeutic targets were identified using the Connectivity Map (CMap) database.

**Results** Five key hub genes—THBD, FOSB, ADGPR3, IL1R2, and PLAUR—were identified as significantly involved in both IBD and AMI pathogenesis. A diagnostic model for AMI constructed using these hub genes demonstrated high predictive accuracy. Single-cell sequencing analysis and several potential drugs targeting these hub genes were identified, offering new therapeutic avenues.

**Conclusion** This study highlights the crucial role of FOSB and other hub genes in the comorbidity of IBD and AMI. The findings provide novel insights for early diagnosis and potential therapeutic strategies, emphasizing the importance of further investigation into these genetic links.

**Keywords** Inflammatory bowel disease, Acute myocardial infarction, Bioinformatics, Machine learning, FOSB, Experimental validation

<sup>†</sup>Qingan Fu, Tianzhou Shen, and Weihan Qiu contributed equally to this article as co-first authors.

\*Correspondence:  
Miao Yu  
happy\_yumiao@163.com

Yue Zhou  
zhouyue2024@yeah.net

<sup>1</sup>Cardiovascular Medicine Department, The Second Affiliated Hospital of Nanchang University, Nanchang 330006, Jiangxi, China

<sup>2</sup>School of Computer Science, South China Normal University, Guangzhou, China



Inflammatory bowel disease (IBD) is a gastrointestinal disorder characterized by chronic inflammation of the gastrointestinal tract and persistent immune system disorders. IBD can be divided into two main types: Crohn's disease (CD) and ulcerative colitis (UC) [1]. Globally, IBD affects more than 6.8 million people, with the United States having the highest age-standardized incidence of 464.5 per 100,000 people, followed by the United Kingdom at 449.6 per 100,000 people [2]. However, in recent years, the incidence of IBD has continued to rise in newly industrialized countries, such as those in Asia, Africa and South America, further burdening the world's health care systems [3].

In addition, parenteral manifestations of IBD are also common and dangerous to patients' health, with cardiovascular disease, malignant tumors, and respiratory disease being the main parenteral factors leading to death in IBD patients [4]. Among the parenteral cardiovascular manifestations of IBD, acute myocardial infarction (AMI) is the most prevalent and serious complication, and AMI is one of the leading cause of death, disability, and reduced quality of life in the world population [5, 6]. In a population-based controlled study, patients with IBD were three times more likely to have a complication of AMI than were healthy individuals, and the findings held after adjusting for variables such as sex and age [7]. In another study involving the prognosis of patients with IBD, the results showed a significant increase in all-cause mortality and the rate of recurrent cardiovascular events in patients with IBD who had experienced an AMI [8]. The occurrence of AMI not only affects the prognosis of patients with IBD but also imposes a heavy financial burden on patients, and further studies on the potential linking mechanisms are urgently needed to reduce the probability of such complications and improve the prognosis of patients.

Available studies have shown that IBD mediates the development of AMI by accelerating the process of atherosclerosis mainly through inflammation and immune system abnormalities. In IBD, mucosal macrophages secrete large amounts of proinflammatory factors, such as IL-1b, IL-6, IL-23, and tumor necrosis factor (TNF), and the increased expression of dendritic cells also increases the secretion of IL-6 and IL-12 [9, 10]. Increased levels of IL-12/IL-23 shift the *in vivo* immune response to an inflammatory T-cell pathway mediated by Th17 and Th1 responses, which are thought to act synergistically to accelerate atherosclerosis [11, 12]. Prolonged inflammation leads to a hypercoagulable state in the blood and an increase in the mean platelet volume (MPV), leading to increased platelet activation and arterial thromboembolic events [13]. In addition, smoking status, changes in intestinal flora, malabsorption of nutrients leading to vitamin B6 deficiency and elevated

homocysteine levels in patients with IBD may also contribute to the development of AMI [15–19]. To date, the biological mechanisms of IBD and AMI are inconclusive, and further in-depth and multifaceted studies are needed to provide additional evidence.

In recent years, with the advancement of bioinformatics and machine learning methods, an increasing number of studies have used bioinformatics and machine learning to analyze the potential mechanism of action of diseases. In this study, we first downloaded IBD- and AMI-related microarray datasets from the NCBI Gene Expression Omnibus (GEO) public database, used enrichment analysis and weighted gene co-expression network analysis (WGCNA) methods to identify genes that are differentially expressed between IBD and AMI and their main functions. The genes obtained in the first two steps were intersected and further screened for hub genes using a machine learning approach. A nomogram was constructed to evaluate the diagnostic efficacy of the hub genes, and the differences in the expression of the hub genes between the AMI patients and controls were also verified via qRT-PCR and western blotting (WB). On the basis of the hub genes, we explored the associations of the hub genes with autophagy, immunity, coagulation, iron death-related genes and immune cell infiltration. Finally, SPIDE3 was also used to search the CMap database for drugs that may antagonize the link between IBD and AMI, and the expression profiles of the hub genes in single-cell samples from AMI patients were evaluated. Hopefully, our screening of hub genes and additional analyses will provide new evidence for the study of the link between IBD and AMI and possible directions for further in-depth studies.

## Materials and methods

### Data sources

The Series Matrix File data file of GSE3365 was downloaded from the GEO database (<https://www.ncbi.nlm.nih.gov/gds>) [19], where GPL96 is the license for the annotation platform. With 85 patients in the IBD group and 42 patients in the normal group, a total of 127 sets of transcriptome data were included [20]. The GSE66360 [Platform GPL570 [HG-U133\_Plus\_2] Affymetrix Human Genome U133 Plus 2.0 Array] dataset was also obtained from the GEO database and included 49 patients with AMI and 50 healthy individuals [21]. The GSE48060 [Platform GPL570 [HG-U133\_Plus\_2] Affymetrix Human Genome U133 Plus 2.0 Array] dataset, which included 21 controls and 31 AMI patients, served as the validation set [22]. The GSE180678 data file was downloaded for single-cell correlation analysis [23]. The expression profile of cardiac tissue specimens was obtained from explanted hearts of adult patients with ischemic cardiomyopathy undergoing cardiac transplantation. Specific information

about the dataset is available on the online website, and the flow chart of the study is shown in Fig. 1.

### Identification of differentially expressed genes (DEGs)

The limma R package [24] was applied to compare the disease and normal groups. The screening cutoff criteria for DEGs were a P value < 0.05 and a |log fold change (FC)| > 1. The ggplot2 R package was used to generate volcano maps.

### GO, KEGG functional analyses and PPI network of the significant DEGs

To further clarify the potential pathway enrichment and functional annotation associated with the DEGs, Gene Ontology (GO), Kyoto Encyclopedia of Genes and Genomes (KEGG) enrichment analyses and protein–protein interaction (PPI) network construction were performed on the DEGs [25]. GO analysis was performed with the clusterProfiler package [26]. The Metascape database ([www.Metascape.org](http://www.Metascape.org)) was used for annotation and visualization of the DEGs KEGG analysis and PPI network [27]. In the GO enrichment analysis, we sorted

the genes according to the q value to select the top 10 genes.

### WGCNA modules and module-trait analysis

WGCNA is often used to identify hub genes in a network as well as to study the relationship between gene networks and disease phenotypes. The top 10,000 genes with the highest variance in the IBD and AMI datasets were identified using the WGCNA-R package; based on this, WGCNA was performed [28]. To evaluate network connectivity, the weighted adjacency matrix was converted to a topological overlap matrix (TOM), and its clustering tree structure was constructed using a hierarchical clustering approach. The branches of the clustering tree represent different gene modules, and the colors represent the individual modules. Based on the gene expression profile data, the WGCNA network matrix was further constructed. The soft-threshold power of  $\beta$  ( $R^2 = 0.85$ ) was set to 2 and 11 for IBD and AMI, respectively, and the minimum module size was 50 to screen the hub modules.

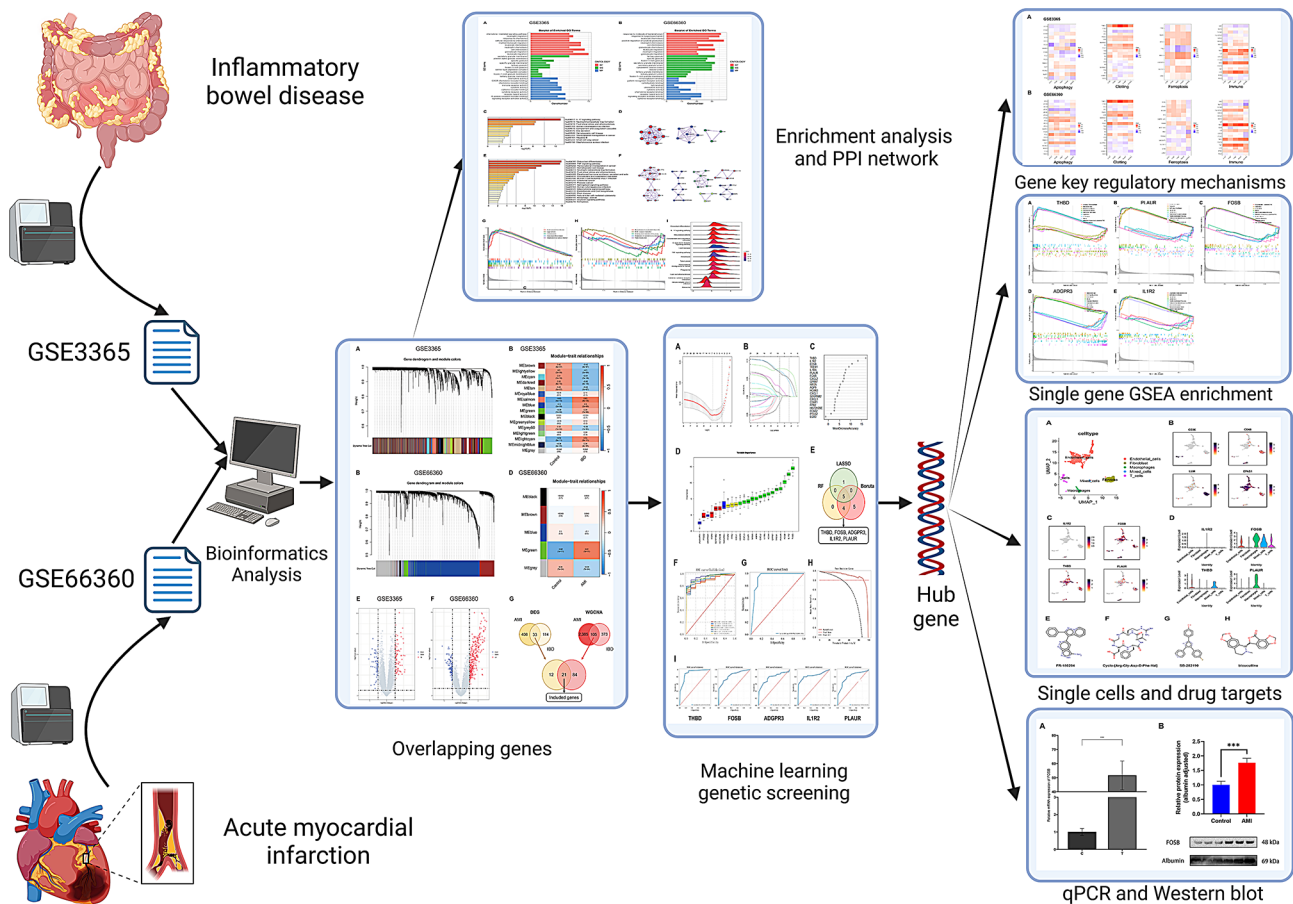


**Fig. 1** Flow chart for multiple bioinformatics analysis and validation

### Machine learning and hub gene screening

First, the intersection of the DEGs and the genes in the WGCNA hub modules were taken as candidate genes. The candidate genes were subsequently screened on this basis using machine learning methods such as the least absolute shrinkage and selection operator (LASSO, glmnet package) algorithm [29], random forest (RF, randomForest package) approach [30, 31], and Boruta approach [32, 33]. The overlapping genes of the obtained results were considered the hub genes of the relationship between IBD and AMI.

### Diagnostic and machine learning model construction

To test the efficacy of the hub genes in predicting the incidence of AMI, we constructed a diagnostic and machine learning model based on random forest using the GSE48060 dataset as a validation set. We plotted ROC curves using the pROC package and examined the diagnostic power of the hub genes using the area under the curve (AUC).

### Single sample gene set enrichment

A single-sample genomic enrichment analysis (ssGSEA) was performed using the clusterProfiler package, which enriched the top five up- and downregulated enrichment terms in the DEGs of AMI patients as well as the hub genes.

### Potential gene-targeted drugs

We queried the Connectivity Map 2 (CMap2) database for targeted drugs that may be associated with specific genes by using SPIED3 (<http://www.spied.org.uk/>) [34, 35]. In this study, we uploaded overlapping genes from the DEGs and genes obtained from WGCNA to SPIED3 to predict drugs compounds that may antagonize the underlying pathogenic mechanisms between IBD and AMI.

### Single-cell sequencing analysis

For single-cell data analysis, the scRNA-seq data were filtered by the R package Seurat v4.3 with the following settings: a gene count per cell > 500 and < 4000 and a percentage of mitochondrial genes < 30% [36]. In the dimensionality reduction clustering step, the number of PCs is set to 30. In the FindClusters step, the resolution was set to 0.1. In the RunUMAP step, n.epochs is set to 500, and umap.method is set to umap-learn. A visual depiction of the gene expression patterns was generated through the use of violin plots, whereas uniform manifold approximation and projection (uMAP) plots were generated using Seurat functions, including VlnPlot and FeaturePlot. R software (version 4.2.3) was used for the data analysis, and  $p < 0.05$  was considered to indicate statistical significance.

### qRT-PCR

The experimental samples used in this study were collected from the peripheral blood of eight clinical AMI patients and eight healthy adults from the Second Affiliated Hospital of Nanchang University, Nei. (This study was conducted in accordance with the principles of the Declaration of Helsinki and was approved by the Ethics Committee of the Second Affiliated Hospital of Nanchang University, Ethical Review No. IIT-O-2024-040). Five ml of peripheral venous blood was collected with sodium heparin anticoagulant blood collection tubes. The topmost plasma was obtained after centrifugation at 12,000 rpm/min for 15 min. Total RNA was extracted from the plasma samples. genomic DNA was removed from the RNA samples and RNA was reverse transcribed using PrimeScript FAST RT reagent Kit with gDNA Eraser (TaKaRa, Code No. 092s). tB Green Premix Ex Taq II FAST qPCR was performed using TB Green Premix Ex Taq II FAST qPCR (TaKaRa, Code No. CN830S/A) and a fluorescence quantitative PCR instrument (Eq. 9600, Applied Eastwin, CHINA) for real-time fluorescence quantitative PCR, a total of 40 cycles were performed, and the mean + standard error of three independent experiments were calculated and each experiment was repeated three times.

### Western blot

The total protein in plasma was extracted by the plasma protein extraction kit (Solarbio, EX1170). After determination of the concentration, equal samples per lane were loaded and separated by SDS-PAGE, followed by transfer onto PVDF membranes. After blocking with 5% fat-free milk powder in TBST buffer, after which the membranes were incubated overnight at 4°C with the following primary antibodies: 1:1000 rabbit anti-human FOSB (CST, #2251), 1:500 rabbit (Bioswamp, PAB49027). The excess primary antibodies were washed 3 × 10 min with TBST, after which the membranes were incubated either with 1:5000 HRP Conjugated AffiniPure Goat Anti-Rabbit IgG (H + L) (Boster, BA1055) for 1 h at RT. Finally, the membranes were washed 3 × 10 min with TBST and the protein bands were detected with the Chemiluminescence Reagent Kit (ECL, Protein Tech, PK10003) according to the manufacturer's instructions.

### Statistics analysis

Densitometry analysis of Western Blot (WB) bands was conducted using ImageJ software (1.53t) (<https://imagej.net/ij>). Statistical significance and graph visualization were conducted in RStudio with R (4.2.3) (<https://www.r-project.org/>). The differences between two groups were analysed by Student's t-test. Diagrams were plotted by the R package ggplot2 (3.4.1) and ggprism (1.0.5). Band intensities were normalized to the loading control, and

the results were expressed as mean ± standard error (SE). \*, \*\* and \*\*\* represent for  $P < 0.05$ ,  $P < 0.01$  and  $P < 0.001$  respectively.

**Results**

**DEGs in the GSE3365 and GSE66360 datasets**

The GSE3365 and GSE66360 datasets were used in the present study to obtain DEG genes for IBD and AMI,

respectively. We set the screening criteria for both P values  $< 0.05$  and  $|\logFC| > 1$ . Finally, 87 upregulated and 60 downregulated genes were obtained from GSE3365, and 332 upregulated and 107 downregulated genes were obtained from GSE66360. Subsequently, we took the intersection of the genes with high and low expression obtained from the two datasets and ultimately obtained 33 DEGs (Fig. 2E, F, G).

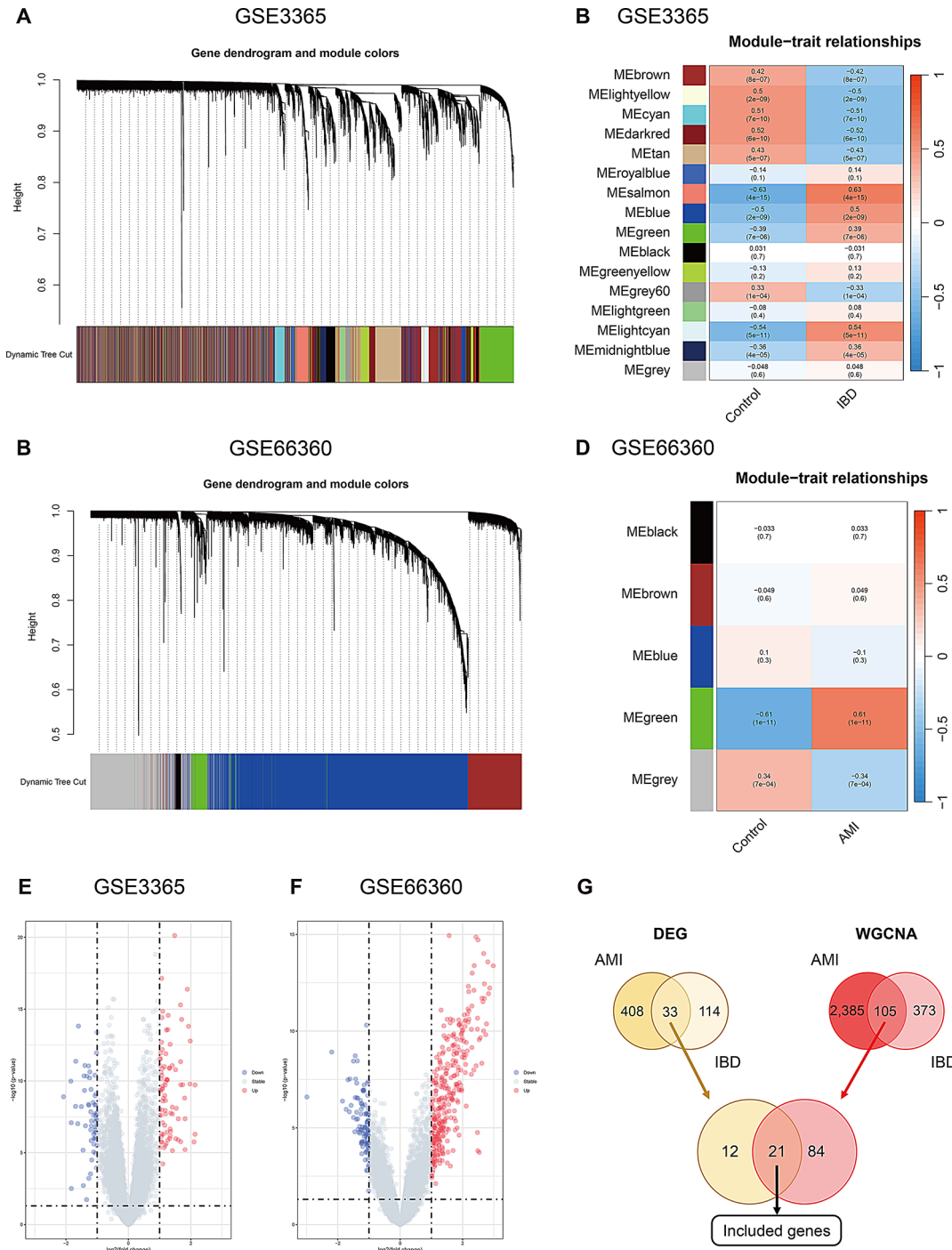


**Fig. 2** WGCNA, volcano and Venn diagrams were screened for DEG genes that were co-expressed or under-expressed in IBD and AMI

### Enrichment analysis and PPI network

We performed multiple pathway enrichment analyses on the DEGs obtained. GO enrichment analysis revealed that GSE3365 was enriched mainly in “cellular chemotaxis”, “chemokine-mediated signaling pathway”, and “myeloid leukocyte”. The enrichment pathway of GSE66360 mainly encompasses positive cytokine regulation, response to bacterial-derived molecules, and cell chemotaxis. According to the results of the KEGG enrichment analysis, the GSE3365 and GSE66360 datasets were coenriched for Neutrophil Extracellular Trap Formation, Fluid Shear Stress and Atherosclerosis, and Complement and Coagulation Cascades pathways, which may be intrinsic to the association of IBD with AMI. Finally, according to the ssGSEA, the DEGs in GSE66360 were predominantly enriched in the C-type lectin receptor signaling pathway, complement and coagulation cascade reactions, and the IL-17 signaling pathway (Fig. 3A, B, C, E, G, H, I). PPI interaction networks highlight the interrelationships and functional modules among different proteins, with each cluster representing a highly interconnected group. These networks reveal the key roles of proteins in the pathogenesis of IBD and AMI, primarily involving mechanistic pathways such as inflammation, immunity, transcriptional regulation, and extracellular matrix remodeling.

### Overlapping genes of IBD and AMI according to WGCNA

First, we constructed IBD-related gene co-expression networks based on the GSE3365 dataset for WGCNA. After setting the thresholds and using the TOM matrix to identify gene modules, we obtained 16 modules: brown(2205), lightyellow(97), cyan(238), darkred(864), tan(1783), royalblue(87), salmon(287), blue(1150), green(806), black(1094), greenyellow(690), gray60(154), lightgreen(133), lightcyan(193), midnightblue(231), gray(4). Among all the modules, salmon ( $\text{cor}=0.63$ ,  $p=4e-15$ ) and lightcyan ( $\text{cor}=0.54$ ,  $p=5e-11$ ) had the strongest correlations with IBD. Similarly, in the WGCNA of the GSE66360 dataset, we obtained a total of five gene modules, namely, black (141), brown (1341), blue (6031), green (422) and gray (2070) (Fig. 2A, B, C, D). Among them, the green module ( $\text{cor}=0.61$ ,  $p=1e-11$ ) had the strongest correlation between the corresponding genes and the disease. Finally, by taking the intersection of the genes identified from the WGCNA with the strong IBD and AMI correlation module, we obtained 105 common strongly correlated genes.

### Identification of hub genes

Making use of the intersection of the 33 DEGs with the 105 common genes obtained from WGCNA yielded 21 genes for machine learning. We then used three machine learning methods, LASSO, RF, and Boruta

to further screen the hub genes. LASSO screened the top 6 genes (PLAUR, ADGPR3, IL1R2, THBD, FOSB, PTGS2) in terms of importance (Fig. 4A, B); RF screened the top 9 genes (THBD, IL1R2, FOSB, TREM1, IL1RN, PLAUR, FCAR, CXCL2, ADGPR3) with importance scores greater than 5 (Fig. 4C); and Boruta screened 14 genes (HCAR3, CXCL3, C5AR1, NRG1, AQP9, CXCL2, IL1RN, FCAR, ADGPR3, TREM1, PLAUR, FOSB, IL1R2, THBD) (Fig. 4D). After overlapping the results obtained from the three methods, we obtained 5 genes—THBD, FOSB, ADGPR3, IL1R2, PLAUR—and used them as the final hub genes for a series of subsequent analyses (Fig. 4E). In addition, the results revealed that the five hub genes all had extremely high individual predictive abilities for AMI, with the test set ROC values of THBD, FOSB, ADGPR3, IL1R2, and PLAUR being 0.905(95%CI=0.743-1.000), 0.841(95%CI=0.636-1.000), 0.781(95%CI=0.521-1.000), 0.839(95%CI=0.616-1.000), and 0.798(95%CI=0.546-1.000), respectively (Fig. 4I).

### Diagnostic model construction

To further establish the pivotal role of the five hub genes in the linkage between IBD and AMI, we built on hub genes to create a diagnostic machine learning model of AMI (The external validation set data is shown in Supplementary Table 1). We used 7 machine learning methods (XGBoost, logistics, LightGBM, RF, SVM, Adaboost and KNN) to build prediction models, among which RF method had the highest prediction accuracy (Fig. 4F). According to the RF for diagnosing AMI patients in the GSE48060 external validation dataset, the area under the curve (AUC) was as high as 0.938, which indicates extremely high diagnostic accuracy (Fig. 4G, H).

### Relationships between hub genes and genes related to key regulatory mechanisms

To investigate the correlation of five key genes with autophagy, coagulation, iron death, and immune aspects in IBD and AMI, we downloaded and analyzed relevant data from the GeneCards database. The results revealed that the five hub genes in GSE3365 and GSE66360 strongly correlated with both coagulation and immunity, while the associations with autophagy and iron death were not significant (Fig. 5). Subsequently, in order to explore the mechanism of action of the five hub genes in the onset of AMI, we further performed GSEA single gene enrichment analysis. The results showed that these hub genes were significantly involved in key cellular metabolism and repair pathways, including lipid metabolism, oxidative stress response and nucleotide repair mechanism, which provided strong evidence to support their important role in AMI (Fig. 6).

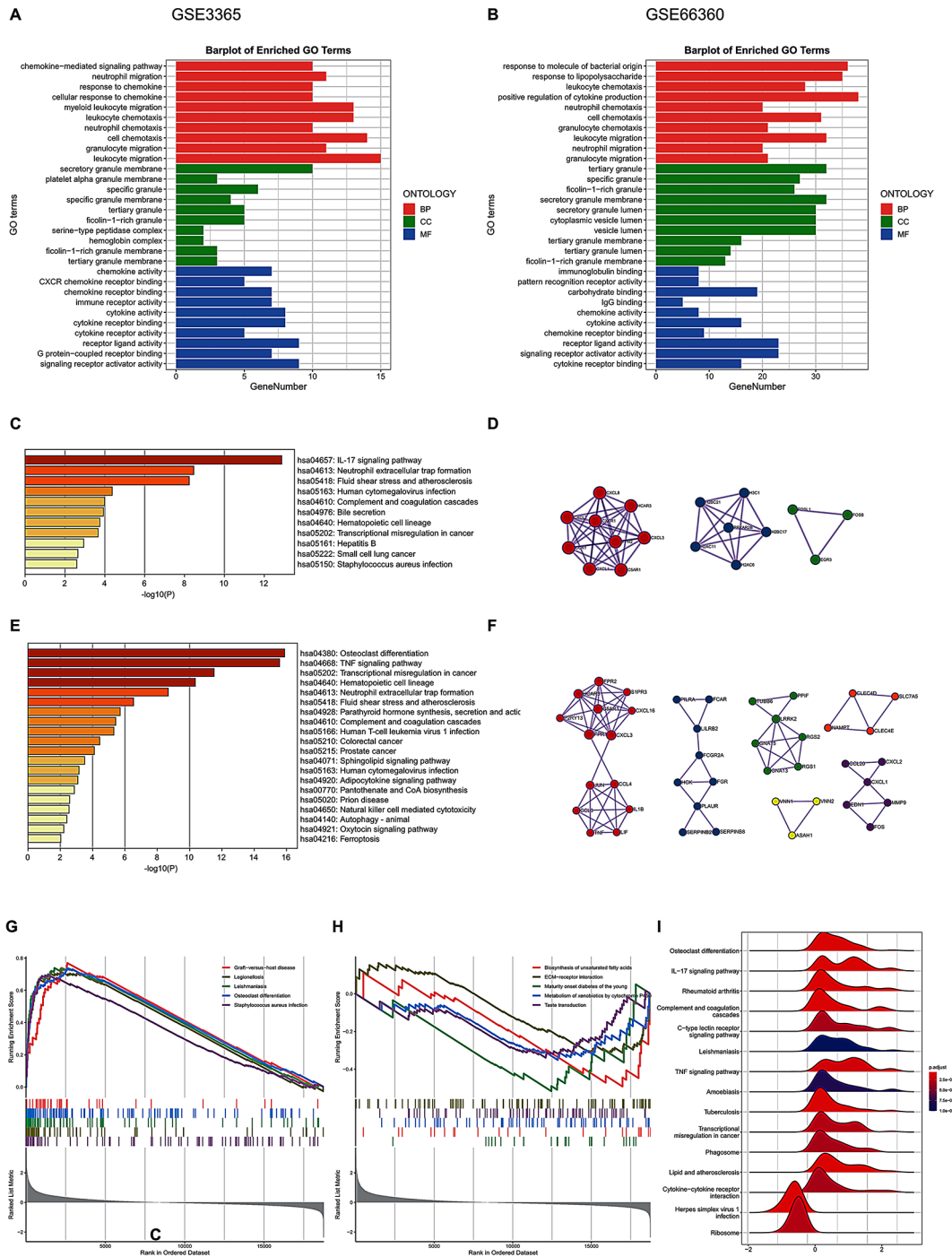


**Fig. 3** GO, KEGG, ssGSEA enrichment analysis of DEG genes and PPI interaction network

**Prediction of targeted drugs compounds**

SPIDE3 was used to identify possible target drugs bud genes, and ultimately, we selected the four drugs with the strongest negative correlation ( $col < -0.95$ ): penbutolol, terazosin, scriptaid, and alfuzosin. The negative correlation exhibited by these drugs suggested that they may be able to prevent or attenuate AMI symptoms induced by

IBD, and their molecular structures are shown in Fig. 7E, F, G, H.

**Overview of hub gene expression in single cells**

We performed single-cell analysis of the downloaded GSE180678 dataset using the Seurat package, and the results of dimensionality reduction clustering using a uMAP plot are shown in Fig. 7A. Each cluster was

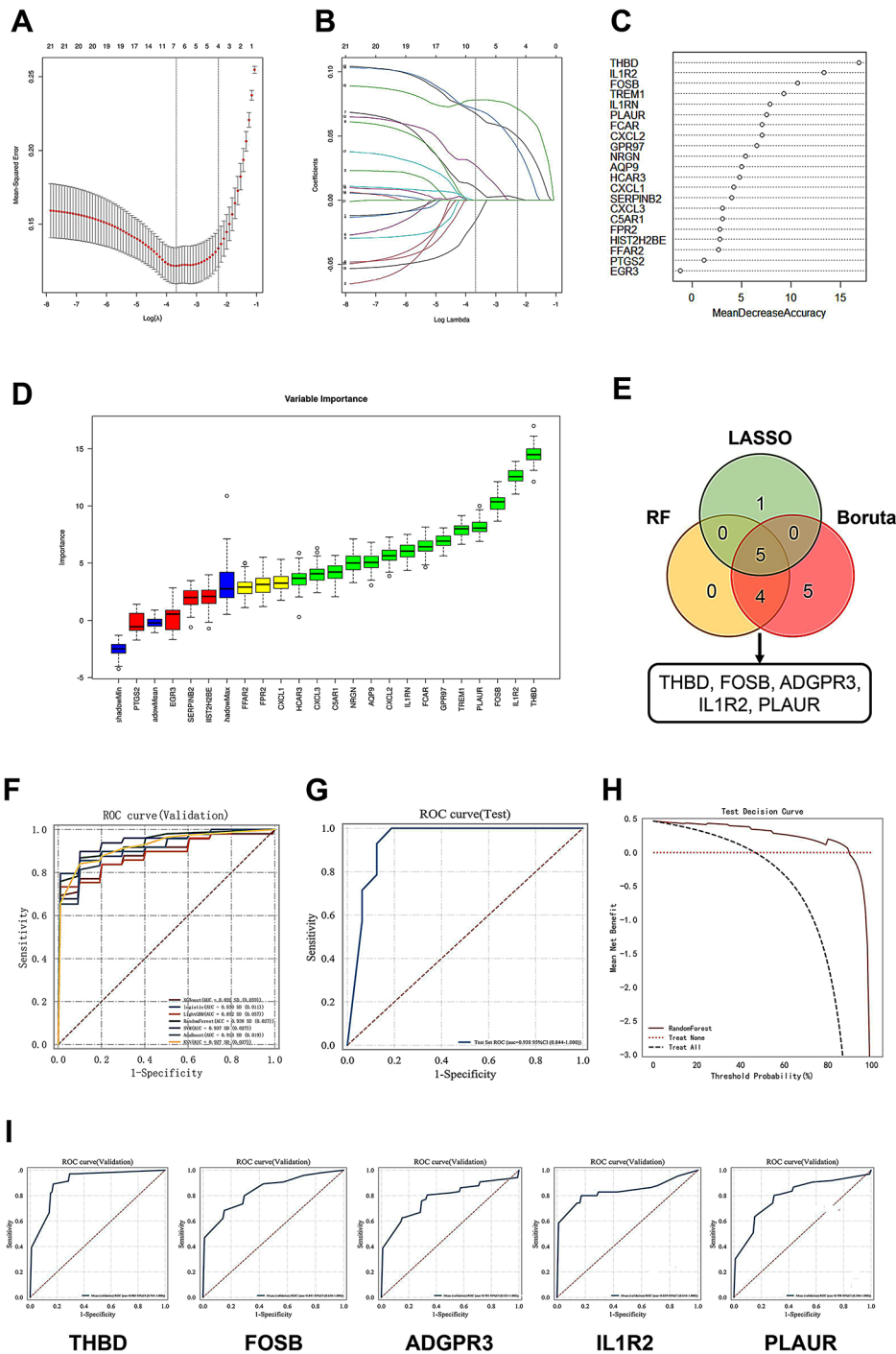
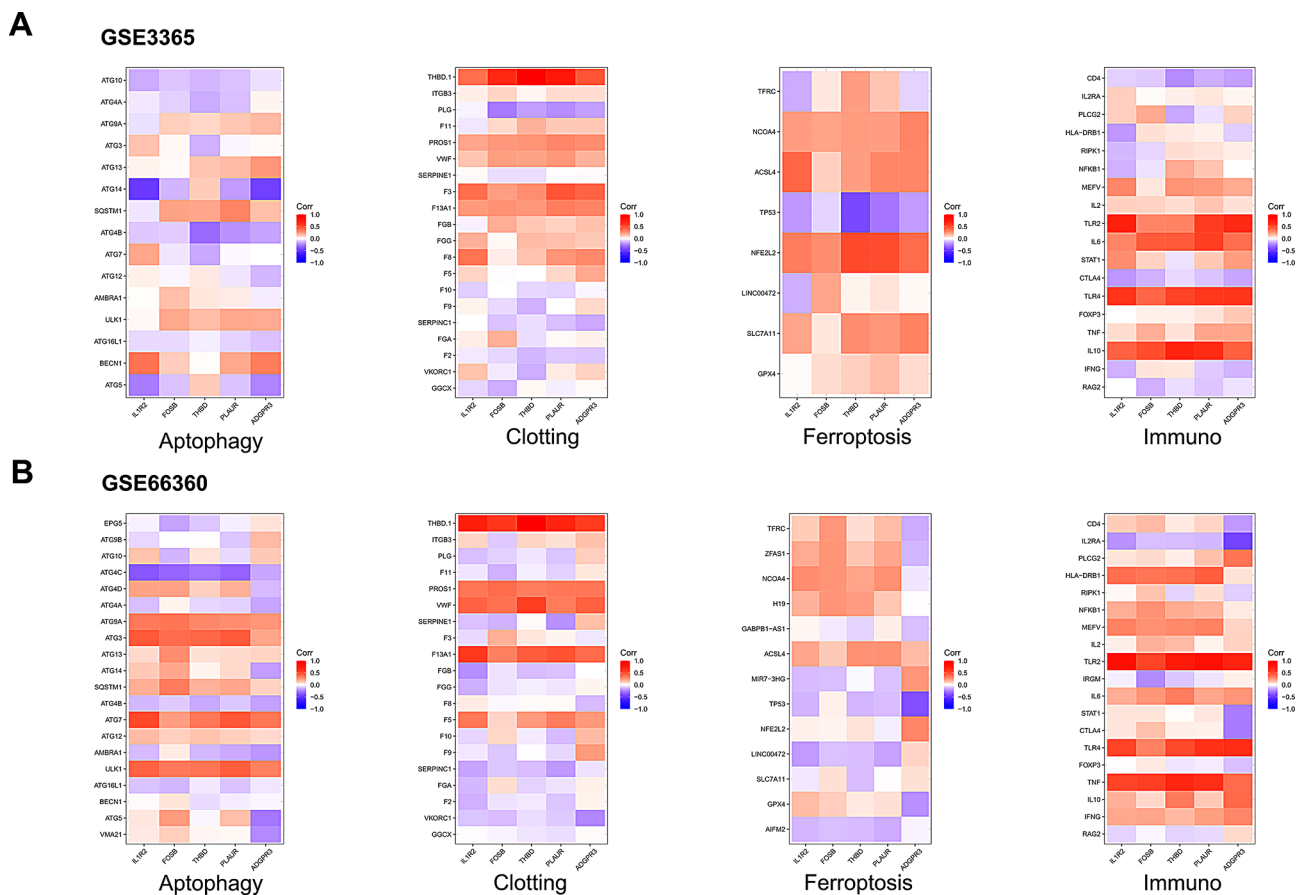


**Fig. 4** LASSO, Boruta and Random Forest methods were used to screen hub genes from DEG genes, and model construction and external validation were performed in GSE48060 based on hub genes

annotated according to the genes that were specifically expressed in each cluster. CD3E, CD68, LUM, and EPSA1 are considered to be markers of T cells, macrophages, fibroblasts, and endothelial cells, respectively (Fig. 7B). The expression levels of THBD, FOSB, ADGPR3, IL1R2 and PLAUR in the four types of cells are shown in the Fig. 7C, D.

**Verification of human blood samples from hub genes**

We collected blood samples from eight AMI patients and eight control volunteers, and then performed qRT-PCR analysis and Western blot analysis based on the blood samples to explore the differences in FOSB between AMI patients and healthy people. The validation results showed that the gene transcription and expression levels



of FOSB in AMI patients were significantly higher than those in the healthy control group, which was consistent with our previous analysis results. (Fig. 8)

## Discussion

IBD is a chronic disease characterized by intestinal inflammation and immune system disorders, and AMI is one of the main and most common causes of death in the general population. Available evidence suggests a strong association between IBD and AMI, which is a common extraintestinal response to IBD; however, the underlying mechanisms are inconclusive, and effective prevention and treatment measures are lacking. In this study, we explored the intrinsic mechanism of the association between IBD and AMI from a bioinformatics point of view. Our analysis yielded five hub genes that may play key roles in IBD and AMI, small molecule drugs that may inhibit this association, and corresponding in vitro experiments to validate the hub gene differences. Ultimately, we verified significantly higher expression of the FOSB gene and its regulated proteins in the AMI population using qRT-PCR and western blot. The findings of this study could lead to the use of new evidence from multiple perspectives in the study of the comorbidity mechanisms

of IBD and AMI, which is of great clinical significance for the early prevention and treatment of AMI events in patients with IBD.

In this study, we first performed multiple bioinformatics analyses based on microarray datasets of IBD and AMI patients to identify DEGs common to both diseases. This kind of multi-omics research combining multiple analytical methods is widely used in the study of disease mechanism and the prediction of pathogenesis, and has already achieved excellent results in the field of tumor prognosis research [37]. Multi-omics research can not only analyze clinical laboratory indexes and imaging data, but also combine bioinformatics analysis and basic experimental validation to explore the intrinsic correlation of different diseases, which is the original intention of our research design [38]. According to the GO enrichment analysis of the DEGs, the IBD-associated DEGs were involved mainly in fundamental processes such as cellular chemotaxis and chemokine-mediated signaling pathways, whereas the AMI DEGs were enriched in cytokine regulation, response to bacterial-derived molecules, and cell chemotherapy. responses to bacterial-derived molecules and cell chemotaxis, the results suggest that chemokine-related pathways may have important roles in

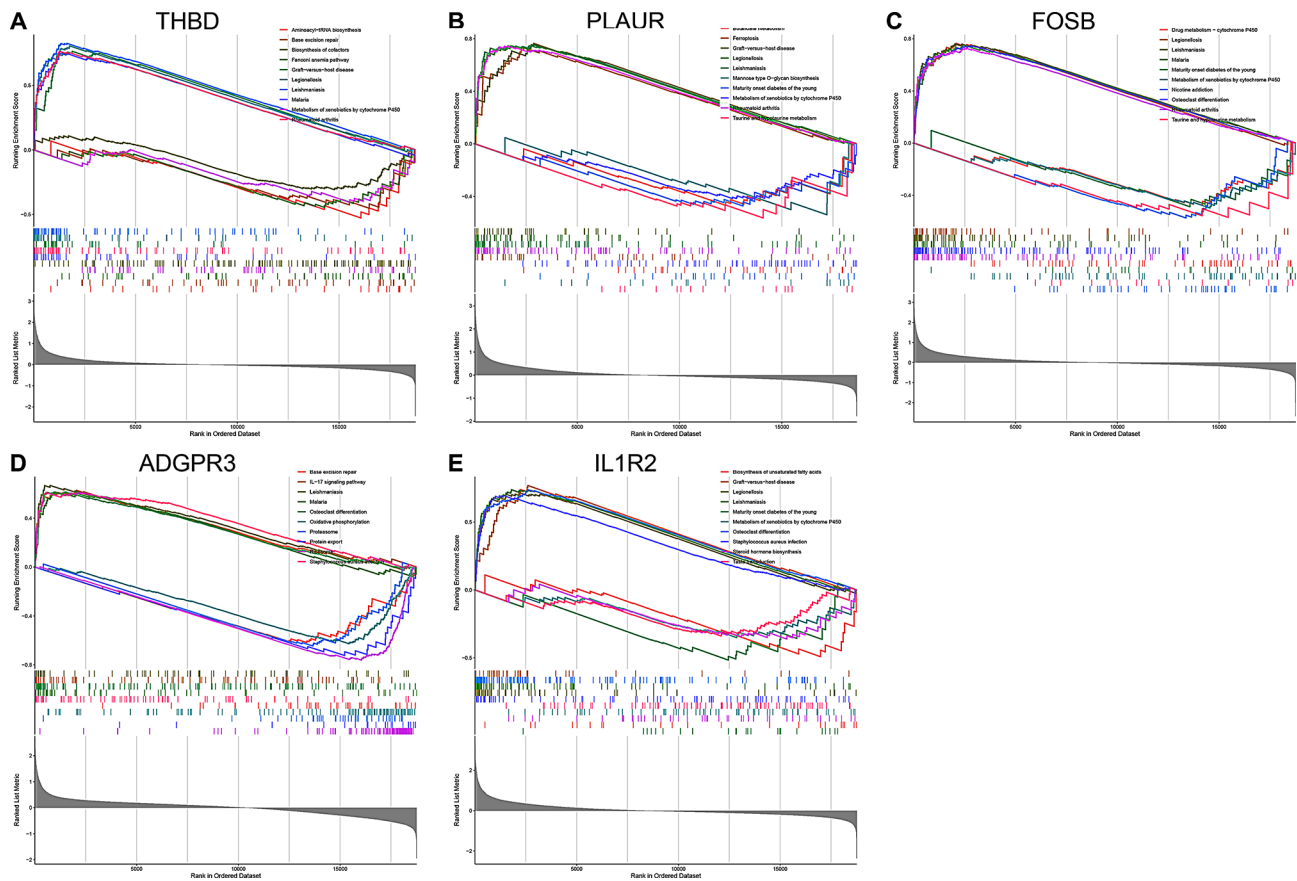


**Fig. 6** GSEA single gene pathway enrichment analysis of five hub genes, THBD, FOSB, ADGPR3, IL1R2 and PLAUR

the development of both diseases. Existing studies have shown that systemic inflammation is a major causative factor in the pathogenesis of a wide range of diseases, and researchers have observed a significant correlation between systemic inflammation indices and poorer prognosis in tumor populations, being a key predictor of death in patients with lung invasive mucinous adenocarcinoma [39]. Similarly, the systemic inflammatory state, represented by chemokine activation, is the most important pathogenic factor in the internal environment of patients with IBD and AMI, and may be a potential mechanism of comorbidity. KEGG analysis demonstrated that the DEGs associated with IBD and AMI act through common pathways, fluid shear stress and atherosclerosis, as well as complement and coagulation cascade pathways. IBD often causes a systemic inflammatory response, which in turn affects the function of vascular endothelial cells and accelerates the development of atherosclerosis. Inflammatory states can also lead to the activation of coagulation factors in the blood, which increases the risk of thrombosis and may be associated with the development of AMI through abnormalities in the coagulation cascade. In addition to inflammation, immune dysfunction is also critical to the pathogenesis of

IBD, and the onset of an immune response can further exacerbate intestinal inflammation. Patients with IBD have an activated immune system, and the complement system is part of the immune response. An overactivated complement system may further exacerbate the inflammatory response, ultimately leading to the development of AMI. Some findings suggest that the acute phase response protein family of SAAs promotes the differentiation of Th17 cells *in vivo* in mesenteric lymph nodes, which in turn mediates the upregulation of IL-17 cytokines and contributes to the development of IBD and that drugs targeting the inhibition of IL-17 have also been observed to be highly efficacious in patients with IBD [40, 41]. Moreover, IL-17 is involved in a variety of inflammatory responses and may also play an important role in the inflammatory environment of AMI. NF- $\kappa$ B is a transcription factor that regulates the systemic inflammatory system and may induce diseases such as IBD and AMI in humans. In animal models, the NF- $\kappa$ B pathway is directly associated with intestinal inflammation. Moreover, during intestinal cancer development, the overexpression of NF- $\kappa$ B is thought to be associated with treatment resistance, advanced tumor stage and poor prognosis. Moreover, activation of p65, the main component of NF- $\kappa$ B, in

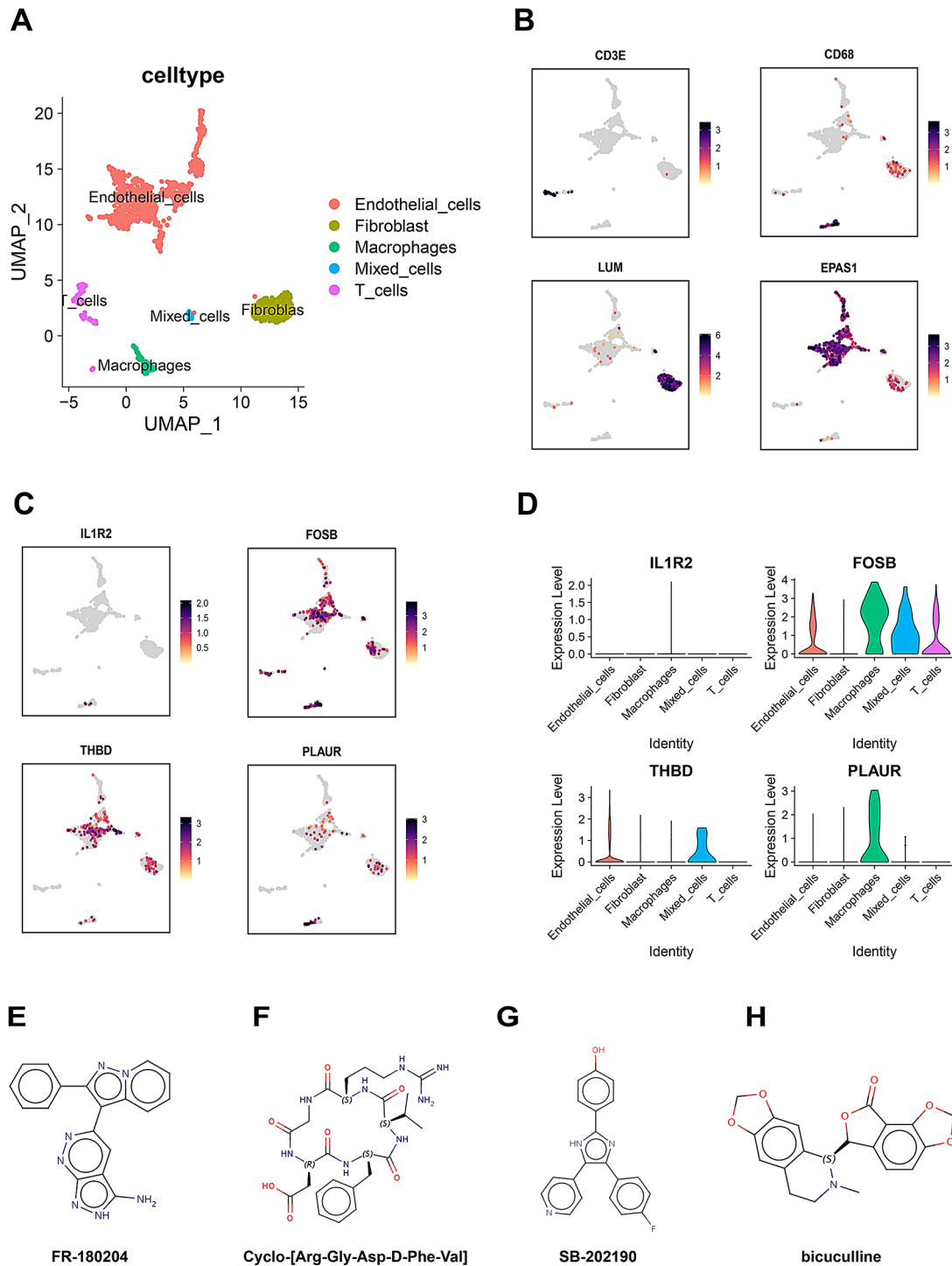


**Fig. 7** Single-cell validation of five hub genes and potential targeting agents

colorectal cancer patients leads to poor clinical outcomes and liver metastasis, fully demonstrating the crucial role of NF- $\kappa$ B in various intestinal diseases [42, 43]. In another study in AMI rats, Lingbao Huxin Pill was able to significantly downregulate the expression of NF- $\kappa$ B p65 and inhibit inflammation and apoptosis in the infarct border zone [44]. The results of various enrichment

analyses fully support the role of IBD-induced risk factors in accelerating the development of AMI, revealing diverse pathogenic factors and pathways involved in comorbid mechanisms.

In addition, important modules and genes that may be shared by IBD patients and AMI patients were identified through the WGCNA co-expression network.

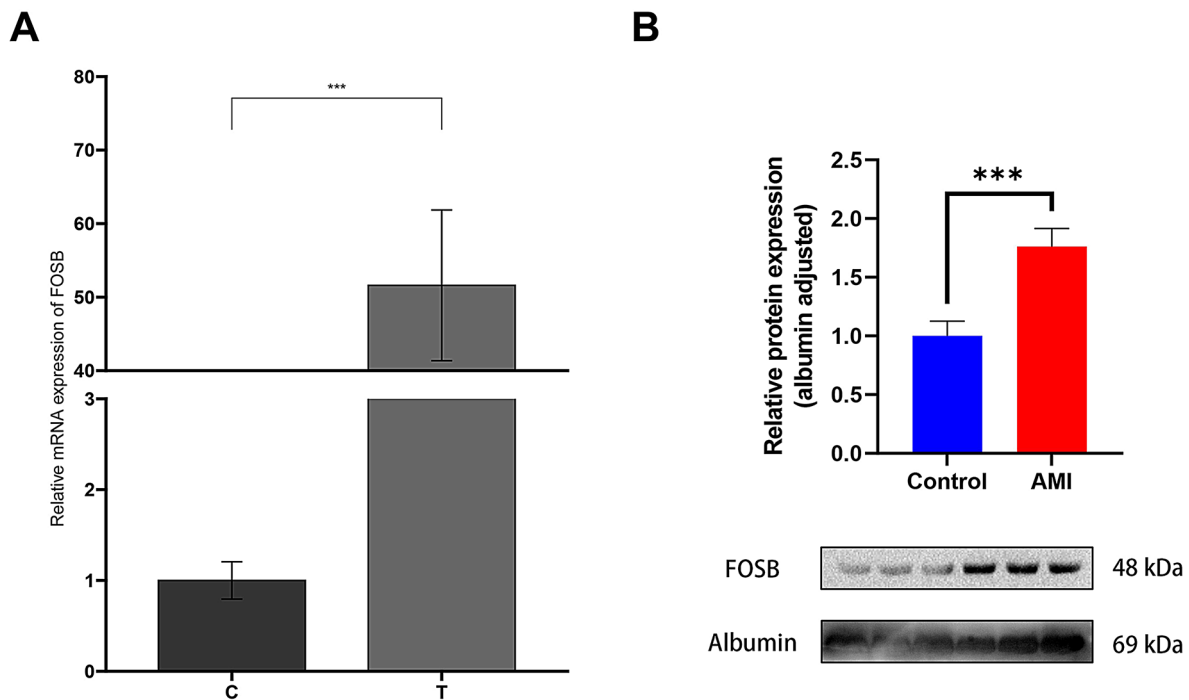


**Fig. 8** Validation of FOSB in human blood samples by qRT-PCR and western blot experiments

Compared with traditional bioinformatics methods, WGCNA focuses on the linkage between clinical features and co-expression modules, which makes the findings more reliable and biologically meaningful. After taking the intersection of the obtained WGCNA genes with 33 DEGs, 5 hub genes were ultimately screened using LASSO, RF and Boruta methods: THBD, FOSB, ADGPR3, IL1R2 and PLAUR for further analysis. We constructed a machine learning diagnostic model for AMI using the five genes, and each gene and the total model demonstrated high prediction accuracy, suggesting that all five hub genes have important roles in the pathogenesis of AMI. IL1R2, a member of the interleukin-1 (IL-1) family, influences immune and inflammatory responses by regulating IL-1 signaling and is also considered a susceptibility locus for IBD. In IBD, excessive IL-1 signaling and the regulation of IL1R2 are associated with chronic inflammation of the intestinal mucosa [45]. In AMI, the inflammatory response is an important piece of the puzzle, and the IL-1-mediated inflammatory milieu leads to a variety of pathological changes, while IL-1R2 has been shown to be associated with atherosclerosis [46, 47]. PLAUR encodes the urokinase-plasminogen activator receptor (uPAR). Existing studies have identified PLAUR as a key gene that regulates matrix metalloproteinases (MMPs), affects cell migration and tissue remodeling, indicating its potential in reducing infarct size and improving cardiac function [48]. Specific single nucleotide polymorphisms in the PLAUR gene have been shown to be associated with increased susceptibility to

myocardial infarction, highlighting the importance of PLAUR in the pathogenesis of myocardial infarction and its impact on personalized medicine [49]. In addition, soluble urokinase plasminogen activators can interact with PLAUR, regulate anti-inflammatory and fibrinolytic pathways that are critical in the treatment of AMI, affect thrombosis and plaque stability, and increase the opportunity for therapeutic intervention in AMI patients [50].

Thrombomodulin, the protein encoded by THBD, is involved in the regulation of blood coagulation and inflammation and is expressed mainly on the surface of vascular endothelial cells [51]. The role of this gene is currently mentioned mainly in AMI, where abnormal coagulation caused by mutations in the THBD gene is the main cause of thromboembolic disease, and the abnormal formation of thrombi ultimately leads to AMI [46]. In the experimental validation of this study, the expression level of FOSB in AMI patients was significantly higher than that in the healthy control group in both qRT-PCR and western blot. FOSB is a member of the AP-1 family of transcription factors and plays a key role in cell cycle regulation, gene regulation, and cell signaling [52]. The results of this study showed that it plays a significant role in AMI, but the specific mechanism is still unclear. There may be several explanations for the increased expression of FOSB in AMI: FOSB responds to oxidative stress by promoting antioxidant enzymes, regulates inflammatory cytokines (such as TNF- $\alpha$ , IL-6, and IL-1 $\beta$ ) to regulate inflammation, and maintains a balance between cell survival and apoptosis to limit infarct size [53]. FOSB also

affects cardiac tissue remodeling by regulating extracellular matrix components and fibrotic reactions [54]. In addition, it participates in signal transduction pathways such as MAPK/ERK and JNK, which are crucial for stress response, and is upregulated by hypoxia-inducible factors (HIFs) under hypoxic conditions, promoting angiogenesis and compensating for blocked blood vessels to improve symptoms [54]. Our results reveal that FOSB may be a new therapeutic target for AMI, and the use of targeted drugs to upregulate the expression of FOSB in patients may improve patient prognosis. Ultimately our study identified four potential therapeutic agents for penbutolol, terazosin, scriptaid, and alfuzosin that may have a preventive effect against AMI by targeting FOSB and thus. Penbutolol is a common drug in the beta-blocker class that is often used clinically to lower blood pressure to control ventricular rate. Although no studies have shown that penbutolol can directly treat AMI or reduce the risk, it may improve the prognosis of AMI patients by activating sympathetic nerves to reduce heart rate, prolonging blood perfusion time, and decreasing myocardial oxygen demand, thereby reducing myocardial ischemic injury [55]. Terazosin, an  $\alpha$ -1 adrenergic receptor blocker, is also commonly used in the clinic for hypotensive therapy, and a recent web-based pharmacologic study suggests that it may be able to be used in the treatment of AMI, which is consistent with our findings [56]. Despite the lack of direct mechanistic studies of terazosin in the treatment of AMI, some studies have demonstrated an improvement in fasting blood glucose and glycosylated hemoglobin levels in terazosin hypertensive patients [57]. Serum total cholesterol and triglyceride levels, which are risk factors for the development of AMI, have been significantly reduced, and terazosin has also been found to have anti-vascular stiffness and aging properties [58]. Scriptaid, an antitumor drug with anti-tumor properties, has recently been found to inhibit the inflammatory response in the nervous system and protect brain function after ischemic injury by promoting microglia differentiation into M2 microglia, but its role in the pathogenesis of AMI remains unclear and requires further study in the future [59, 60]. Finally, alfuzosin is often used as a symptomatic treatment for prostatic hypertrophy and hypertension, and is an  $\alpha$ 1-adrenergic antagonist. Researchers have found that alfuzosin activates PGK1 to stimulate the protein kinase B signaling pathway, glucose uptake and improves insulin resistance, which in turn reduces the risk of diabetes mellitus, one of the high-risk factors for AMI [61]. Additionally, alfuzosin was found to have a delayed myocardial repolarization effect, which may allow for more adequate myocardial perfusion in AMI patients, again providing an explanation for its potential role in treating AMI [62].

The immune system is an important part of the disease process in both IBD and AMI, microbial and environmental factors interact with the host [63]. In AMI, immune mediators such as M1 proinflammatory macrophages and M2 reparative macrophages continue to act at all stages of the disease process [64]. First, the classical monocyte pathway promotes innate immune responses through direct action and indirect differentiation into dendritic cells. Similarly, monocytes have also been shown to play an important role in the activation of adaptive immune responses through antigen presentation to T cells. Only early depletion of monocytes in AMI increases cellular necrosis, and later, monocytes play a key role in ventricular remodeling after AMI, suggesting that both monocyte-mediated early inflammatory processes and late repair are essential for infarct healing [64]. Some researchers have shown an increase in monocytes, macrophages, and neutrophils in the mucosa of patients with IBD, which may be associated with tissue homing, further suggesting that these cellular infiltrates may be associated with the severity of IBD [65]. Mast cells (MCs) were found to mediate FXR in animal experiments, leading to increased intestinal FXR/FGF15 expression and exacerbated intestinal inflammation in IBD patients [66]. MC hyperreactivity has also been viewed as a risk factor for altered gut function in IBD patients, which may be caused by dysregulated interactions between the microbiota and MC [67]. In addition, our study identified four potential small molecule drugs targeting the hub gene, which may provide a new therapeutic direction from a bioinformatics perspective, and additional studies are needed in the future for specific efficacy validation.

We downloaded a single-cell dataset to explore the expression of the hub gene within different subpopulations of cells in single cells, providing multidimensional evidence for the study. Single-cell analysis revealed that the hub genes were predominantly enriched in monocyte, macrophage, and endothelial cell subpopulations in AMI patients. Cellular immunity training mechanisms and systemic inflammation in monocytes may lead to elevated splenic tyrosine kinase (SYK) expression, which ultimately mediates the development of atherosclerosis (AS) and AMI in both AMI patients and mice, whereas mice deficient or depleted of macrophages or monocytes were observed to have a lower probability of developing AS. In addition, trained immunity occurs not only in immune cells but also in endothelial cells and smooth muscle cells, both of which can induce AS formation [68]. These findings suggest that monocytes, macrophages, and endothelial cells all play important roles in the development of AMI, consistent with our findings.

Although previous studies have shown that IBD patients have a greater risk of AMI, few studies have explored the comorbidity mechanism between these two

diseases from the perspective of bioinformatics methods. In this study, we identified and explored the common hub genes associated with two diseases, analyzed the potential regulatory factors associated with these hub genes. These findings provide evidence from multiple perspectives for further investigations of the comorbidity mechanisms of IBD and AMI. This study has the following limitations. First, only 5 hub genes were identified in this study; the distribution of hub genes in the human body was not determined, and the full genetic profile of the disease could not be represented, as the disease completely mimics IBD and AMI. Second, additional data on the clinical characteristics of the patients should be included in this study for further subgroup analyses. Finally, although qPCR and WB confirmed the high expression of FOXB in AMI patients, there is still a lack of basic experimental studies at the cellular or animal level exploring the effect of overexpression or knockdown of FOXB on AMI risk. Moreover, the potential drugs targeting IBD-AMI identified in this study were not subjected to corresponding pharmacological experiments to verify their efficacy due to the limitations of experimental conditions, and more specific functional and targeted therapeutic drug experiments are needed to further validate our findings in animal experiments and clinical studies in the future.

## Conclusion

In this study, we evaluated the transcriptomic data of IBD and AMI patients via bioinformatics methods, identified the hub genes associated with these two diseases, constructed a diagnostic model, evaluated the association and pathogenesis of IBD and AMI through functional enrichment of the hub genes, screening of drug targets, immune infiltration, single-cell sequencing, qPCR, WB analysis. The results suggest that the precise diagnosis and treatment of IBD and AMI can be realized in the future through the modulation of inflammation, coagulation, and immune-related factors, but these findings still need to be verified by further animal and clinical experiments.

## Supplementary Information

The online version contains supplementary material available at <https://doi.org/10.1186/s12920-025-02129-0>.

Supplementary Material 1

Supplementary Material 2

Supplementary Material 3

## Acknowledgements

We thank the participants who provided blood samples and the public database workers and designers. We also thank Biorender for help with the drawings.

## Author contributions

QF: wrote the main manuscript text. TS and WQ: data analysis. YL: western blot. MY: prepared supplementary material. YZ: data analysis and revise the manuscript. All authors reviewed the manuscript.

## Funding

This research was funded by Natural Science Foundation of Jiangxi Province - Youth Fund Project (No. 20212BAB216045, 20224BAB216013) and the National Natural Science Foundation of China - Regional Program (No. 82360083).

## Data availability

No datasets were generated or analysed during the current study.

## Declarations

### Ethics approval and consent to participate

All GEO data are public, the original research has been reviewed by the ethics committee, and all participants have signed informed consent. The patients from whom the blood sample data came have signed informed consent, and this study was conducted in accordance with the principles of the Declaration of Helsinki (<https://www.wma.net/policies-post/wma-declaration-of-helsinki/>) and was approved by the Institutional Review Board Ethics Committee of the Second Affiliated Hospital of Nanchang University, Ethical Review No. IIT-O-2024-040. More information about the data can be obtained by contacting the corresponding author.

### Consent for publication

Not applicable.

### Competing interests

The authors declare no competing interests.

Received: 12 February 2025 / Accepted: 20 March 2025

Published online: 03 April 2025

## References

1. Ananthakrishnan AN. Epidemiology and risk factors for IBD. *Nat Rev Gastroenterol Hepatol*. 2015;12(4):205–17.
2. The global, regional, and National burden of inflammatory bowel disease in 195 countries and territories, 1990–2017: a systematic analysis for the global burden of disease study 2017. *Lancet Gastroenterol Hepatol*. 2020;5(1):17–30.
3. Ng SC, Shi HY, Hamidi N, Underwood FE, Tang W, Benchimol EI, Panaccione R, Ghosh S, Wu JCY, Chan FKL, et al. Worldwide incidence and prevalence of inflammatory bowel disease in the 21st century: a systematic review of population-based studies. *Lancet*. 2017;390(10114):2769–78.
4. Olén O, Askling J, Sachs MC, Neovius M, Smedby KE, Ekblom A, Ludvigsson JF. Mortality in adult-onset and elderly-onset IBD: a nationwide register-based cohort study 1964–2014. *Gut*. 2020;69(3):453–61.
5. Singh A, Museedi AS, Grossman SA. Acute Coronary Syndrome. In: *StatPearls*. Treasure Island (FL): StatPearls Publishing. Copyright. © 2023, StatPearls Publishing LLC.; 2023
6. Rungoe C, Nyboe Andersen N, Jess T. Inflammatory bowel disease and risk of coronary heart disease. *Trends Cardiovasc Med*. 2015;25(8):699–704.
7. Aniwaniwan S, Pardi DS, Tremaine WJ, Loftus EV Jr. Increased risk of acute myocardial infarction and heart failure in patients with inflammatory bowel diseases. *Clin Gastroenterol Hepatol*. 2018;16(10):1607–e16151601.
8. Kristensen SL, Ahlehoff O, Lindhardtsen J, Erichsen R, Lamberts M, Khalid U, Nielsen OH, Torp-Pedersen C, Gislason GH, Hansen PR. Prognosis after first-time myocardial infarction in patients with inflammatory bowel disease according to disease activity: nationwide cohort study. *Circ Cardiovasc Qual Outcomes*. 2014;7(6):857–62.
9. Kamada N, Hisamatsu T, Okamoto S, Chinen H, Kobayashi T, Sato T, Sakuraba A, Kitazume MT, Sugita A, Koganei K, et al. Unique CD14 intestinal macrophages contribute to the pathogenesis of Crohn disease via IL-23/IFN-gamma axis. *J Clin Invest*. 2008;118(6):2269–80.
10. Hart AL, Al-Hassi HO, Rigby RJ, Bell SJ, Emmanuel AV, Knight SC, Kamm MA, Stagg AJ. Characteristics of intestinal dendritic cells in inflammatory bowel diseases. *Gastroenterology*. 2005;129(1):50–65.

11. Yen D, Cheung J, Scheerens H, Poulet F, McClanahan T, McKenzie B, Kleinschek MA, Owyang A, Mattson J, Blumenschein W, et al. IL-23 is essential for T cell-mediated colitis and promotes inflammation via IL-17 and IL-6. *J Clin Invest*. 2006;116(5):1310–6.
12. Baumer Y, Dey AK, Gutierrez-Huerta CA, Khalil NO, Sekine Y, Sanda GE, Zhuang J, Saxena A, Stempinski E, Elnabawi YA, et al. Hyperlipidaemia and IFN $\gamma$ /TNF $\alpha$  synergism are associated with cholesterol crystal formation in endothelial cells partly through modulation of lysosomal pH and cholesterol homeostasis. *EBioMedicine*. 2020;59:102876.
13. Dogan Y, Soylu A, Eren GA, Poturoglu S, Dolapcioglu C, Sonmez K, Duman H, Sevindir I. Evaluation of QT and P wave dispersion and mean platelet volume among inflammatory bowel disease patients. *Int J Med Sci*. 2011;8(7):540–6.
14. Halfvarson J, Brislawn CJ, Lamendella R, Vázquez-Baeza Y, Walters WA, Bramer LM, D'Amato M, Bonfiglio F, McDonald D, Gonzalez A, et al. Dynamics of the human gut Microbiome in inflammatory bowel disease. *Nat Microbiol*. 2017;2:17004.
15. Lykkesfeldt J, Christen S, Wallock LM, Chang HH, Jacob RA, Ames BN. Ascorbate is depleted by smoking and repleted by moderate supplementation: a study in male smokers and nonsmokers with matched dietary antioxidant intakes. *Am J Clin Nutr*. 2000;71(2):530–6.
16. Biedermann L, Fournier N, Misselwitz B, Frei P, Zeitz J, Manser CN, Pittet V, Juillerat P, von Känel R, Fried M, et al. High rates of smoking especially in female Crohn's disease patients and low use of supportive measures to achieve smoking Cessation—Data from the Swiss IBD cohort study. *J Crohns Colitis*. 2015;9(10):819–29.
17. Saibeni S, Cattaneo M, Vecchi M, Zighetti ML, Lecchi A, Lombardi R, Meucci G, Spina L, de Franchis R. Low vitamin B(6) plasma levels, a risk factor for thrombosis, in inflammatory bowel disease: role of inflammation and correlation with acute phase reactants. *Am J Gastroenterol*. 2003;98(1):112–7.
18. D'Angelo A, Mazzola G, Crippa L, Fermo I, Viganò D'Angelo S: hyperhomocysteinemia and venous thromboembolic disease. *Haematologica*. 1997;82(2):211–9.
19. Barrett T, Wilhite SE, Ledoux P, Evangelista C, Kim IF, Tomashevsky M, Marshall KA, Phillippy KH, Sherman PM, Holko M, et al. NCBI GEO: archive for functional genomics data sets—update. *Nucleic Acids Res*. 2013;41(Database issue):D991–995.
20. Palmer NP, Silvester JA, Lee JJ, Beam AL, Fried I, Valtchinov VI, Rahimov F, Kong SW, Ghodoussipour S, Hood HC, et al. Concordance between gene expression in peripheral whole blood and colonic tissue in children with inflammatory bowel disease. *PLoS ONE*. 2019;14(10):e0222952.
21. Muse ED, Kramer ER, Wang H, Barrett P, Parviz F, Novotny MA, Lasken RS, Jatko TA, Oliveira G, Peng H, et al. A whole blood molecular signature for acute myocardial infarction. *Sci Rep*. 2017;7(1):12268.
22. Suresh R, Li X, Chiriac A, Goel K, Terzic A, Perez-Terzic C, Nelson TJ. Transcriptome from Circulating cells suggests dysregulated pathways associated with long-term recurrent events following first-time myocardial infarction. *J Mol Cell Cardiol*. 2014;74:13–21.
23. DeBerge M, Lantz C, Dehn S, Sullivan DP, van der Laan AM, Niessen HWM, Flanagan ME, Brat DJ, Feinstein MJ, Kaushal S et al. Hypoxia-inducible factors individually facilitate inflammatory myeloid metabolism and inefficient cardiac repair. *J Exp Med* 2021, 218(9).
24. Ritchie ME, Phipson B, Wu D, Hu Y, Law CW, Shi W, Smyth GK. Limma powers differential expression analyses for RNA-sequencing and microarray studies. *Nucleic Acids Res*. 2015;43(7):e47.
25. Kanehisa M, Goto S. KEGG: Kyoto encyclopedia of genes and genomes. *Nucleic Acids Res*. 2000;28(1):27–30.
26. Yu G, Wang LG, Han Y, He QY. ClusterProfiler: an R package for comparing biological themes among gene clusters. *Omic*. 2012;16(5):284–7.
27. Zhou Y, Zhou B, Pache L, Chang M, Khodabakhshi AH, Tanaseichuk O, Benner C, Chanda SK. Metascape provides a biologist-oriented resource for the analysis of systems-level datasets. *Nat Commun*. 2019;10(1):1523.
28. Langfelder P, Horvath S. WGCNA: an R package for weighted correlation network analysis. *BMC Bioinformatics*. 2008;9:559.
29. Vasquez MM, Hu C, Roe DJ, Chen Z, Halonen M, Guerra S. Least absolute shrinkage and selection operator type methods for the identification of serum biomarkers of overweight and obesity: simulation and application. *BMC Med Res Methodol*. 2016;16(1):154.
30. Paul A, Mukherjee DP, Das P, Gangopadhyay A, Chintha AR, Kundu S. Improved random forest for classification. *IEEE Trans Image Process*. 2018;27(8):4012–24.
31. Fu Q, Wu Y, Zhu M, Xia Y, Yu Q, Liu Z, Ma X, Yang R. Identifying cardiovascular disease risk in the U.S. Population using environmental volatile organic compounds exposure: A machine learning predictive model based on the SHAP methodology. *Ecotoxicol Environ Saf*. 2024;286:117210.
32. Speiser JL, Miller ME, Tooze J, Ip E. A comparison of random forest variable selection methods for classification prediction modeling. *Expert Syst Appl*. 2019;134:93–101.
33. Wang H, Fu Q, Xiao S, Ma X, Liao Y, Kang C, Yang R. Predictive value of the triglyceride-glucose index for short- and long-term all-cause mortality in patients with critical coronary artery disease: a cohort study from the MIMIC-IV database. *Lipids Health Dis*. 2024;23(1):263.
34. Subramanian A, Narayan R, Corsello SM, Peck DD, Natoli TE, Lu X, Gould J, Davis JF, Tubelli AA, Asiedu JK, et al. A next generation connectivity map: L1000 platform and the first 1,000,000 profiles. *Cell*. 2017;171(6):1437–e14521417.
35. Williams G. SPIEDw: a searchable platform-independent expression database web tool. *BMC Genomics*. 2013;14(1):765.
36. Stuart T, Butler A, Hoffman P, Hafemeister C, Papalexi E, Mauck WM 3rd, Hao Y, Stoeckius M, Smibert P, Satija R. Comprehensive integration of Single-Cell data. *Cell*. 2019;177(7):1888–e19021821.
37. Ye B, Jiang A, Liang F, Wang C, Liang X, Zhang P. Navigating the immune landscape with plasma cells: A pan-cancer signature for precision immunotherapy. *BioFactors*. 2025;51(1):e2142.
38. Ye B, Fan J, Xue L, Zhuang Y, Luo P, Jiang A, Xie J, Li Q, Liang X, Tan J: iMLGAM: Integrated Machine Learning and Genetic Algorithm-driven Multiomics analysis for pan-cancer immunotherapy response prediction. *iMeta* 2025:e70011.
39. Sun W, Zhang P, Ye B, Situ MY, Wang W, Yu Y. Systemic immune-inflammation index predicts survival in patients with resected lung invasive mucinous adenocarcinoma. *Transl Oncol*. 2024;40:101865.
40. Lee JY, Hall JA, Kroehling L, Wu L, Najar T, Nguyen HH, Lin WY, Yeung ST, Silva HM, Li D, et al. Serum amyloid A proteins induce pathogenic Th17 cells and promote inflammatory disease. *Cell*. 2020;180(1):79–e9116.
41. Moschen AR, Tilg H, Raine T. IL-12, IL-23 and IL-17 in IBD: immunobiology and therapeutic targeting. *Nat Rev Gastroenterol Hepatol*. 2019;16(3):185–96.
42. Berkovich L, Gerber M, Katzav A, Kidron D, Avital S. NF- $\kappa$ B expression in resected specimen of colonic cancer is higher compared to its expression in inflammatory bowel diseases and polyps. *Sci Rep*. 2022;12(1):16645.
43. Nissim-Eliraz E, Nir E, Marsiano N, Yagel S, Shpigel NY. NF- $\kappa$ B activation unveils the presence of inflammatory hotspots in human gut xenografts. *PLoS ONE*. 2021;16(5):e0243010.
44. Tan Y, Bie YL, Chen L, Zhao YH, Song L, Miao LN, Yu YQ, Chai H, Ma XJ, Shi DZ. Lingbao Huxin pill alleviates apoptosis and inflammation at infarct border zone through SIRT1-Mediated FOXO1 and NF- $\kappa$ B pathways in rat model of acute myocardial infarction. *Chin J Integr Med*. 2022;28(4):330–8.
45. Lees CW, Barrett JC, Parkes M, Satsangi J. New IBD genetics: common pathways with other diseases. *Gut*. 2011;60(12):1739–53.
46. Zhao E, Xie H, Zhang Y. Predicting diagnostic gene biomarkers associated with immune infiltration in patients with acute myocardial infarction. *Front Cardiovasc Med*. 2020;7:586871.
47. Peters VA, Joesting JJ, Freund GG. IL-1 receptor 2 (IL-1R2) and its role in immune regulation. *Brain Behav Immun*. 2013;32:1–8.
48. Yu YW, Xue YJ, Qian LL, Chen Z, Que JQ, Huang KY, Liu S, Weng YB, Rong FN, Ji KT, et al. Screening and identification of potential hub genes in myocardial infarction through bioinformatics analysis. *Clin Interv Aging*. 2020;15:2233–43.
49. Xu J, Li W, Bao X, Ding H, Chen J, Zhang W, Sun K, Wang J, Wang X, Wang H, et al. Association of putative functional variants in the PLAU gene and the PLAU gene with myocardial infarction. *Clin Sci (Lond)*. 2010;119(8):353–9.
50. Hindy G, Tyrrell DJ, Vasbinder A, Wei C, Presswala F, Wang H, Blakely P, Ozel AB, Graham S, Holton GH et al. Increased soluble urokinase plasminogen activator levels modulate monocyte function to promote atherosclerosis. *J Clin Invest* 2022, 132(24).
51. Manderstedt E, Halldén C, Lind-Halldén C, Elf J, Svensson PJ, Engström G, Melander O, Baras A, Lotta LA, Zöller B. Thrombomodulin (THBD) gene variants and thrombotic risk in a population-based cohort study. *J Thromb Haemost*. 2022;20(4):929–35.
52. Dougherty EJ, Elinoff JM, Ferreyra GA, Hou A, Cai R, Sun J, Blaine KP, Wang S, Danner RL. Mineralocorticoid receptor (MR) trans-Activation of inflammatory AP-1 signaling: DEPENDENCE ON DNA SEQUENCE, MR CONFORMATION, AND AP-1 FAMILY MEMBER EXPRESSION. *J Biol Chem*. 2016;291(45):23628–44.
53. Alfonso-Jaume MA, Bergman MR, Mahimkar R, Cheng S, Jin ZQ, Karliner JS, Lovett DH. Cardiac ischemia-reperfusion injury induces matrix metalloproteinase-2 expression through the AP-1 components FosB and JunB. *Am J Physiol Heart Circ Physiol*. 2006;291(4):H1838–1846.

54. Khachigian LM. Transcription factors targeted by MiRNAs regulating smooth muscle cell growth and intimal thickening after vascular injury. *Int J Mol Sci* 2019;20(21).
55. Wong GW, Wright JM. Blood pressure Lowering efficacy of nonselective beta-blockers for primary hypertension. *Cochrane Database Syst Rev*. 2014;2014(2):Cd007452.
56. Barbieri MA, Abate A, Balogh OM, Pétervári M, Ferdinandy P, Ágg B, Battini V, Cocco M, Rossi A, Carnovale C et al. Network Analysis and Machine Learning for Signal Detection and Prioritization Using Electronic Healthcare Records and Administrative Databases: A Proof of Concept in Drug-Induced Acute Myocardial Infarction. *Drug Saf* 2025.
57. Zhang C, Li J, Wang L, Ma J, Li X, Wu Y, Ren Y, Yang Y, Song H, Li J, et al. Terazosin, a repurposed GPR119 agonist, ameliorates mitophagy and  $\beta$ -cell function in NAFLD by inhibiting MST1-Foxo3a signalling pathway. *Cell Prolif*. 2025;58(3):e13764.
58. Guan Y, Zhang Y, Chen L, Ren Y, Nie H, Ji T, Yan J, Zhang C, Ruan L. Effect of low-dose Terazosin on arterial stiffness improvement: A pilot study. *J Cell Mol Med*. 2024;28(14):e18547.
59. Sanchez-Martin V, Ruzic D, Tello-Lopez MJ, Ortiz-Morales A, Murciano-Calles J, Soriano M, Nikolic K, Garcia-Salcedo JA. The histone deacetylase inhibitor Scriptaid targets G-quadruplexes. *Open Biol*. 2025;15(2):240183.
60. Meng Q, Yang G, Yang Y, Ding F, Hu F. Protective effects of histone deacetylase Inhibition by Scriptaid on brain injury in neonatal rat models of cerebral ischemia and hypoxia. *Int J Clin Exp Pathol*. 2020;13(2):179–91.
61. Zhou J, Wu T, Li C, Hu Z, Han L, Li X, Liu J, Zhao W, Kang J, Chen X. Alifuzosin ameliorates diabetes by boosting PGK1 activity in diabetic mice. *Life Sci*. 2023;317:121491.
62. Lacerda AE, Kuryshev YA, Chen Y, Renganathan M, Eng H, Danthi SJ, Kramer JW, Yang T, Brown AM. Alifuzosin delays cardiac repolarization by a novel mechanism. *J Pharmacol Exp Ther*. 2008;324(2):427–33.
63. Glassner KL, Abraham BP, Quigley EMM. The Microbiome and inflammatory bowel disease. *J Allergy Clin Immunol*. 2020;145(1):16–27.
64. Peet C, Ivetic A, Bromage DI, Shah AM. Cardiac monocytes and macrophages after myocardial infarction. *Cardiovasc Res*. 2020;116(6):1101–12.
65. Mitsialis V, Wall S, Liu P, Ordovas-Montanes J, Parmet T, Vukovic M, Spencer D, Field M, McCourt C, Toothaker J, et al. Single-Cell analyses of colon and blood reveal distinct immune cell signatures of ulcerative colitis and Crohn's disease. *Gastroenterology*. 2020;159(2):591–e608510.
66. Meadows V, Kennedy L, Ekser B, Kyritsi K, Kundu D, Zhou T, Chen L, Pham L, Wu N, Demieville J, et al. Mast cells regulate ductular reaction and intestinal inflammation in cholestasis through farnesoid X receptor signaling. *Hepatol-ogy*. 2021;74(5):2684–98.
67. De Zuani M, Dal Secco C, Frossi B. Mast cells at the crossroads of microbiota and IBD. *Eur J Immunol*. 2018;48(12):1929–37.
68. Dong Z, Hou L, Luo W, Pan LH, Li X, Tan HP, et al. Myocardial infarction drives trained immunity of monocytes, accelerating atherosclerosis. *Eur Heart J*. 2023;45(9):669–84.

### Publisher's note

Springer Nature remains neutral with regard to jurisdictional claims in published maps and institutional affiliations.